Title

Macrophage and CD8 T cell discordance are associated with acute lung allograft dysfunction progression.

Journal

The Journal of heart transplantation, 43(7)

Authors

Calabrese, Daniel
Ekstrand, Christina
Yellamilli, Shivaram
et al.

Publication Date

2024-07-01

DOI

10.1016/j.healun.2024.02.007

Peer reviewed

HHS Public Access

Author manuscript

J Heart Lung Transplant. Author manuscript; available in PMC 2024 July 08.

Published in final edited form as:

J Heart Lung Transplant. 2024 July ; 43(7): 1074–1086. doi:10.1016/j.healun.2024.02.007.

Macrophage and CD8 T Cell Discordance are Associated with Acute Lung Allograft Dysfunction Progression

Daniel R. Calabrese[1,2], **Shivaram Yellamilli**[3,†], **Christina Ekstrand**[3,†], **Jonathan P. Singer**[1], **Steven R. Hays**[1], **Lorriana E. Leard**[1], **Rupal J. Shah**[1], **Aida Venado**[1], **Nicholas A. Kolaitis**[1], **Alyssa Perez**[1], **Alexis Combes**[3], **John R. Greenland**[1,2]

[1]Department of Medicine, University of California, San Francisco, CA

[2]Medical Service, Veterans Affairs Health Care System, San Francisco, CA.

[3]Department of Pathology, University of California, San Francisco, CA

Abstract

Purpose: Acute lung allograft dysfunction (ALAD) is an imprecise syndrome denoting concern for the onset of chronic lung allograft dysfunction (CLAD). Mechanistic biomarkers are needed that stratify risk of ALAD progression to CLAD. We hypothesized that single cell investigation of bronchoalveolar lavage (BAL) cells at the time of ALAD would identify immune cells linked to progressive graft dysfunction.

Methods: We prospectively collected BAL from consenting lung transplant recipients for single cell RNA sequencing. ALAD was defined by a ≥10% decrease in FEV_1 not caused by infection or acute rejection and samples were matched to BAL from recipients with stable lung function. We examined cell compositional and transcriptional differences across control, ALAD with decline, and ALAD with recovery groups. We also assessed cell-cell communication.

Results: BAL was assessed for 17 ALAD cases with subsequent decline (ALAD declined), 13 ALAD cases that resolved (ALAD recovered), and 15 cases with stable lung function. We observed broad differences in frequencies of the 26 unique cell populations across groups ($p = 0.02$). A CD8 T cell ($p = 0.04$) and a macrophage cluster ($p = 0.01$) best identified ALAD declined from the ALAD recovered and stable groups. This macrophage cluster was distinguished by an anti-inflammatory signature and the CD8 T cell cluster resembled a Tissue Resident Memory subset. Anti-inflammatory macrophages signaled to activated CD8 T cells via class I HLA, fibronectin, and galectin pathways ($p < 0.05$). Recipients with discordance between these cells had a nearly 5-fold increased risk of severe graft dysfunction or death (HR 4.6, 95% CI 1.1–19.2, adjusted $p = 0.03$). We validated these key findings in 2 public genomic datasets.

Conclusions: BAL anti-inflammatory macrophages may protect against CLAD by suppressing CD8 T cells. These populations merit functional and longitudinal assessment in additional cohorts.

Correspondence and reprint requests: Dr. Daniel R. Calabrese, San Francisco VA Health Care System, 4150 Clement St, San Francisco, CA 94121, USA.

†Denotes equal contribution

INTRODUCTION

Lung transplant improves duration and quality of life for patients suffering from advanced lung diseases (1). However, long-term outcomes among lung allograft recipients are worse than in other solid organ allograft recipients (2). The major driver of lung allograft morbidity and mortality is chronic lung allograft dysfunction (CLAD), a clinical syndrome of reduced lung function that occurs in 50% of recipients by 5 years (1, 3). CLAD is diagnosed by the development of an irreversible 20% decline in lung function not attributable to alternate causes including weight gain, airway stenosis, or pleural effusions (4). However, by the time these criteria are met significant small airway structural loss has occurred. Thus, this delayed detection impedes early intervention. It follows that establishing pathologic processes and early biomarkers that precede this decline are imperative(5).

The need for early CLAD diagnosis has prompted proposed terminology for acute decreases in lung allograft function that might presage CLAD, including “incipient CLAD,” “acute lung allograft dysfunction” (ALAD), “acute rejection”, and “acute decline” (6-8). These terms lack consensus definitions and debate exists as to how acute graft infections, cellular and antibody-mediated rejection should be incorporated into this nomenclature. With respect to linking ALAD to molecular drivers, a narrower definition may be more facile. The greatest need is to distinguish signs and symptoms representing early CLAD (ALAD with subsequent decline), from a similar clinical presentation not associated with CLAD pathology (ALAD followed by recovery).

CLAD pathology is described as concentric small airway fibrosis leading to progressive airway obstruction (BOS) or, in the diffuse parenchymal form, pleuroparenchymal fibroelastosis and lung function restriction (RAS) (9-11). There is little evidence that BOS and RAS have distinct molecular drivers, and there are currently few established therapies for either form of CLAD. The pathophysiology of CLAD is multimodal and not clearly established. Small airway injury, through a variety of risk factors and potential mechanisms, leads to exhaustion of the airway progenitor niche (6, 12-15). Eventually, normal airway is replaced by fibrosis. The alloimmune response features prominently in this cascade (16). Several groups have identified increased cytotoxic lymphocytes, including CD8 T cells and natural killer cells, in lung airway or tissue samples of CLAD (6, 15, 17-22). In addition, recent evidence has revealed a role for innate immune involvement via inflammatory interferon stimulated or TGFβ-primed macrophages in CLAD (7, 23).

We hypothesized that single cell investigation of bronchoalveolar lavage (BAL) cells at the time of ALAD would identify immune cell subsets linked to progressive CLAD.

METHODS

Complete detail on all methodological aspects for this study is provided in the data supplement.

Study Design

We prospectively enrolled consenting adult lung transplant recipients who underwent bronchoscopy at the University of California, San Francisco (UCSF) between 1/01/2021 to 6/01/2022. Inclusion and exclusion criteria are shown in Figure 1A. Acute lung allograft dysfunction (ALAD) was defined as a new 10% or greater decrease in FEV_1 from the post-transplant baseline values (4). ALAD samples with concomitant infection or rejection were excluded. Included ALAD participants were matched 2:1 based on age and sample time after transplantation to no-ALAD control participants.

Clinical data, outcomes, protocols

Data were abstracted from medical records, as previously described (24). Participants were characterized as: (1) “no ALAD,” if they did not have an acute decline in lung function at the time of bronchoscopy (2) “ALAD recovered,” if they had a 10% decline in FEV_1 but improved at 1 year follow-up, or (3) “ALAD declined” if the FEV_1 decline did not resolve or the participant died before further measurements. Freedom from stage 2 CLAD was defined as days from bronchoscopy until >40% decline in FEV_1 from baseline or death.

Cellular indexing of transcriptomes and epitopes (CITE) single cell sequencing.

BAL samples were processed and frozen within 6 hours of collection. Thawed, viable cells were pooled, stained for surface markers, and loaded directly in the Chromium Controller for single cell encapsulation with gel bead-in-emulsions (GEMs) per manufacturer’s directions. Reverse transcription, cDNA library generation and sequencing on a NovaSeq6000 (Illumina) were conducted, as described previously (25). The sequenced reads were aligned and processed. We filtered the data, demultiplexed the pools, and normalized to cell state (26). All libraries were combined into a single Seurat object. A UMAP was generated, and cells were clustered by RNA expression using the Louvain Algorithm. We combined similar clusters based on manual assessment of differentially expressed genes and proteins as well as common lineage markers.

Validation approaches in external cohorts

We reanalyzed publicly available microarray data from BAL collected from no CLAD control recipients (n = 8) and at the time of incipient CLAD (n = 9) (6). Cell cluster gene metagene scores were constructed as previously described (27), using the top differentially expressed genes, and we compared cell cluster gene scores between CLAD cases and controls. We also reanalyzed tissue gene expression data from a separate study of CLAD tissue (n = 3) and no CLAD control tissue (n = 1) (28). We manually segmented areas within each sample and graded them as no pathology or CLAD. Log_2 sum gene expression was quantified across these regions of interest.

Statistical analyses

Differences among cohort subject characteristics were compared using 2-tailed Student’s *t*- and χ^2-tests, as appropriate. Comparisons between multiple groups were made using Kruskal-Wallis one-way test and between 2 groups with Mann Whitney U testing.

Differences in clusters of BAL cells between ALAD groupings were determined by PERMANOVA.

We generated a Random Forest machine learning mode to assess the frequency of each cell population as a predictor of ALAD decline. We employed leave one out validation (29), and the model accuracy and fit were assessed through area under the curve receiver operator curve calculations.

We utilized Cox proportional hazards models to test the association between predictors of interest and progression to stage 2 CLAD or death. Event-free survival was visualized with Kapan-Meier methods. Differences between CLAD airways and no-CLAD airways in tissue gene expression analyses were determined by linear regression treating study sample as a random effect to account for repeat measures within samples. All models were adjusted for baseline characteristics (30, 31). *P*-values less than 0.05 were considered significant. Statistical analyses were performed in R (version 4.1.1, R Foundation for Statistical Computing).

RESULTS

Acute lung allograft dysfunction cohort

Over 18 months of recruitment, we identified 58 lung transplant recipients with an acute 10% decrease in FEV_1. Of these, 9 had concurrent pathogenic respiratory infections and 5 had acute cellular rejection (Supplemental Table 1). We matched the remaining recipients to contemporaneous patients without acute lung dysfunction (Figure 1A, Supplemental Table 2). As an internal control, we also analyzed samples obtained from two participants before and during ALAD, for a total of 47 samples across 45 individuals. Baseline characteristics between these 2 groups are shown in Table 1. ALAD and non-ALAD participants had no differences across these variables. Though, non- ALAD samples were collected a median 597 days interquartile range ([IQR], 367 – 728 days) after transplant compared to 753 IQR 445 – 1825 days in the ALAD group.

Figure 1B shows lung function at the time of bronchoscopy and at 1 year follow-up for the cohort. At the time of BAL collection, non-ALAD participants (n = 15) had robust lung function with median FEV_1 of 103% of post-transplant baseline and interquartile range (IQR) 101 – 105%. At 1 year follow-up, these same participants had stable or improved FEV_1 (median 106%, IQR 100 – 111%) compared to baseline values at enrollment. In contrast, the participants with ALAD (n = 30) had a median FEV_1 of 83% (IQR 78 – 89%) of baseline. At 1 year, 17 (57%) of the ALAD participants did not improve or suffered further decline in lung function with median FEV_1 67% (IQR 39 – 78%). Notably, all participants with FEV_1 decline developed CLAD or died by 1 year (Figure 1C). The 3 ALAD recipient deaths were respiratory-related. The remaining 13 ALAD participants recovered or stabilized their lung function with FEV_1 at 1-year median 99% (IQR 94–101%) of post-transplant baseline. Differences between baseline characteristics in ALAD recovered and ALAD declined participants are shown in Supplemental Table 3.

Single cell RNA sequencing identifies broad cell differences across ALAD groups

Having observed this profound decline in participants with ALAD who did not recover, we asked whether this group was associated with a unique BAL cell compositional profile relative to participants with stable or improved lung function. We performed unsupervised clustering of the 51,273 sequenced cells to define distinct cellular populations within the BAL. Twenty-six unique cell populations were identified within this compartment (Figure 2A). Supplemental Figure 1 shows the top differentially expressed genes in each cluster. Notably, 75% of these clusters were macrophages or monocytes. When cluster plots were shaded by 1-year ALAD status (Figure 2B), there were several areas of significant overlap between the control participants and those that developed ALAD but recovered. In contrast, participants with ALAD that declined had distinct differences compared to the other groups. Figure 2C shows bar plots of the frequencies of cells in all clusters for each ALAD group, with distinct cellular landscapes across the 3 groups (Figure 2C, $p = 0.02$).

Lymphocyte and macrophage clusters are different in recipients with progressive ALAD

To determine which specific cell clusters were associated with decline after ALAD, we fit a machine learning models using cell clusters as a predictor of ALAD with decline (Figure 3A). By area under the curve receiver operator curve (AUC ROC) calculations, the model classified ALAD cases with decline (AUC 0.65, 95% confidence interval [CI] 0.5–0.78). Figure 3B shows the relative importance of the top 10 features. Notably, T regulatory cells (Figure 3C, $p = 0.003$), activated CD8 T cells (Figure 3D, $p = 0.02$), anti-inflammatory macrophages (Figure 3E, $p = 0.005$), CD8 T cells (Figure 3F, $p = 0.08$), NK cells (Figure 3G, $p = 0.07$) and a macrophage cluster (Figure 3H, $p = 0.1$) were most reliable to discriminate between ALAD decline and the other groups. Differences in cell proportions for the remaining 20 clusters are shown in Supplemental Figure 2. We found no differences in either of these two cell populations with respect to time after transplant (Supplemental Figure 3) but note a trend for increased activated CD8 T cells over time.

Notably, CD8 T cells and macrophage populations have been previously identified during early CLAD (7, 17). An interferon-stimulated population was not different in this comparison but was increased in ALAD decline as compared to ALAD recovered ($p = 0.02$). Here, we note that anti-inflammatory macrophages are decreased in decline. Thus, we focused on CD8 T cells and anti-inflammatory macrophage groups given their significance in identifying ALAD progression in this cohort and previous interest in the field.

Anti-inflammatory macrophages and activated CD8 T cells have distinct profiles.

To understand the functional role for these cell types in ALAD pathogenesis we examined their defining gene transcripts across the entire cohort. Figure 4A shows the top differentially transcribed genes for anti-inflammatory macrophages with false discovery rate (FDR) p-values < 0.05 stratified by relative fold change. A pathway analysis (Figure 4B) revealed key regulatory functions of this cluster in autophagic cell death, complement and cytokine domains. Notably, this macrophage population does not follow classical categorization by canonical M1 or M2 markers (Supplemental Figure 4).

Transcriptional analysis of the activated CD8 T cells revealed markers of tissue residency and activation (Figure 4C). Pathway analysis suggested these features overlapped with NK cell cytotoxicity and allograft rejection (Figure 4D). An evaluation of surface receptors on this CD8 T cell cluster revealed additional markers of tissue residency and activation (Figure 4E, Supplemental Figure 5) consistent with a tissue resident effector memory CD8 T cells (T_{RM}, Figure 4F) phenotype. Together, we observed reduced anti-inflammatory macrophages and increased in T_{RM} CD8 T cells preceding ALAD progression.

We also assessed if these cell types changed over time. We note that one participant with decline had a pre-ALAD and an ALAD sample that demonstrated decreasing anti-inflammatory macrophages with ALAD (Supplemental Figure 6A) and increasing activated CD8 T cells with ALAD (Supplemental Figure 6B). This contrasts with the participant with recovered ALAD who had decreasing anti-inflammatory macrophages (Supplemental Figure 6C) and activated CD8 T cells during ALAD (Supplemental Figure 6D).

Anti-inflammatory macrophage and CD8 T cell communication network

We next investigated communication across clusters within the entire cohort. We found significant predicted interactions between cell types (Figure 5A). Given our findings, we investigated the direction and strength of cell-cell signals among anti-inflammatory macrophages. This revealed that their strongest signals were sent to CD8 T cells and activated CD8 T cells, and that they were predicted to receive little input from other cells (Figure 5B). In contrast, the 2 CD8 T cell groups largely received signals from all cells in the BAL. Notably, CD8 and activated CD8 T cells were not predicted to send any signals. We next investigated the specific receptor-ligand interactions predicted to feature in signaling between anti-inflammatory macrophages and CD8 T cells. As expected, human leukocyte antigen – CD8 T cell ligand-receptor pairings were predicted to be the dominant interactions between anti-inflammatory macrophages and CD8 T cells (Figure 5C). However, galectin, fibronectin, and chemokine interactions also featured in this communication network. Thus, we identified several plausible pathways whereby anti-inflammatory macrophages may signal to activated CD8 T cells.

Discordance in anti-inflammatory macrophage and activated CD8 T cell populations predict graft failure.

Give our findings that activated CD8 T cells were increased while anti-inflammatory macrophages were decreased preceding ALAD decline as well as a plausible communication pathway between the two cell types, we hypothesized that discordant frequencies would be associated with allograft failure. Among recipients without ALAD progression, we found anti-inflammatory macrophages, and activated CD8 T cells were positively associated ($p < 0.0001$; Figure 6A). However, in ALAD decline, this association was absent ($p = 0.64$). Similarly, we found an increased ratio of activated CD8 T cells to anti-inflammatory macrophages among recipients with ALAD decline (Figure 6B, $p = 0.0002$). Consequently, recipients with high activated CD8 T cells (> median) and low anti-inflammatory macrophages (<median, n = 10) had 4.6-fold increased risk for progressing to stage 2 obstructive CLAD or death (95% CI, 1.1 – 19.2, adjusted $p = 0.03$) compared to

recipients without this cellular discordance (Figure 6C). These findings suggest an important interaction between these two cell populations.

Validation of key findings in 2 lung transplant molecular cohorts.

We sought to validate our key findings in additional lung transplant cohorts. We obtained publicly available microarray data from BAL collected from no CLAD control recipients (n = 8) and at the time of incipient CLAD (n = 9) (6). We constructed gene scores using the top differentially expressed transcripts in the anti-inflammatory macrophage and activated CD8 T cell clusters, displayed as heatmaps in Figure 7A. Notably, the gene score for anti-inflammatory macrophages was decreased in BAL from recipients with incipient CLAD compared to no-CLAD control BAL (Figure 7B, p = 0.04). Activated CD8 T cell signatures were numerically increased in the incipient CLAD group as well (Figure 7C, p = 0.06). Separately, we obtained publicly available tissue gene expression data from another study of CLAD tissue (n = 3) and no CLAD control tissue (n = 1) (28). We measured total gene expression within anatomic segments surrounding airways (Figure 7D). We found that anti-inflammatory macrophage genes were decreased around CLAD airways (Figure 7E, p = 0.005) and activated CD8 T cells were increased around CLAD airways (Figure 7F, p = 0.02) as compared to no-CLAD or early CLAD airways. These findings were adjusted for repeat measures within the same individual.

DISCUSSION

This prospective cohort of lung transplant recipients with ALAD not attributable to infection or acute rejection identified cell compositional changes associated with risk of irreversible and progressive graft dysfunction. As the largest lung transplant BAL single cell RNA sequencing/CITEseq cohort study to date, we were able to identify a key role for a regulatory macrophage population. We further leveraged cell-cell communication networks to identify a macrophage-CD8 T cell interaction with a previously undescribed role in protecting from CLAD progression. We validated these findings in two external lung transplant cohorts at a similar time after transplant. Such cellular interactions may prove to be attractive therapeutic targets.

Similar to prior reports, we identify a striking diversity in the alveolar macrophage population (7). We described nearly 16 transcriptionally distinct macrophage clusters across our cohort, furthering the notion that human airway macrophages cannot be neatly divided across M1/M2 designations (32). We identified a singular population that was increased in BAL in stable participants those with ALAD with recovery of lung function but was notably absent in BAL from ALAD recipients who experienced decline. This alveolar macrophage population had transcriptional programs suggestive of anti-inflammatory or regulatory functions. Notably, genes *SERPING1, LIPA,* and *CCL18* have previously been described in macrophages with anti-inflammatory profiles (33-35). *SERPING1*, has been shown to reprogram macrophages and reduce experimental sepsis associated organ injury (33). Further, *SERPING1* inhibits the complement system which suggests a potential role for this macrophage population in mitigating antibody mediated rejection (36). This population also expressed *CCL18*, which has been shown to bridge the response from inflammation

to resolution of injury (34). Thus, we hypothesize that the absence of the macrophage population may release a critical brake on the airway inflammatory response leading to CLAD.

We identified one population of CD8 T cells that may drive this inflammatory response among ALAD recipients with progression. Activated CD8 T cells and their transcripts have been reported previously in CLAD (6, 22, 28, 37, 38). However, the population identified here, expressed NK cell receptors (DNAM1) and had transcriptional and surface markers of tissue residency (CD49a, CD69, CD103) found in T_{RM} CD8 T cells (39). T_{RM} CD8 T cells are a unique population with antigen-specificity and tissue-residence, situated at the mucosal interface (40). In experimental influenza infection, CXCR6 mediated the localization of T_{RM} cells to the airways (41). Here, we also identified increased CXCR6 in this T_{RM} population, which suggests a potential mechanism whereby these antigen-specific tissue-resident cells hone to the small airways, the site of CLAD pathology. It is worth noting that this population may not correspond perfectly with CD8+ T_{RM} identified by flow cytometry as some transcriptionally similar lymphocyte populations may be clustered together. Snyder and colleagues recently described 3 unique T_{RM} populations within the lung after transplantation with distinct phenotypic and clinical associations (17, 42). Notably, the cellular population we describe here most resembles the cluster of T_{RM}s previously associated with acute rejection, suggesting a role in injury.

These data complement studies showing how macrophages may potentiate the allograft CD8 T cell response. In a TGFβ-dependent fashion, monocyte-derived alveolar macrophages promote experimental BOS airway injury via stimulation of T_{RM} CD8 T cells (23, 43). Indeed, human T_{RM} cells co-localize with alveolar macrophages near small airways (44). Macrophage and T cell crosstalk also feature prominently in other forms of acute lung injury (45). Though, the proportions of BAL macrophages have been reported as decreased during CLAD (46). These changes may be due to increased frequencies of other cells, challenges with immunophenotyping pulmonary macrophages with flow cytometry, or low resolution with traditional approaches (47). With the introduction of scRNA-seq, more detail in this cellular niche has been revealed. Moshkelgosha and colleagues identified 2 distinct macrophage populations during ALAD; an interferon stimulated gene (ISG) macrophage group and a metallothionine (MT) macrophage group (7). Comparable to the ISG macrophage group, we identified a similar macrophage population marked by *CXCL10* and *SOD2* expression that was increased during ALAD that went on to progress relative to ALAD recovered groups. We did not find a MT macrophage population, though other populations in our study may have similar functions. Thus, while this cohort resembled a prior ALAD study in design, these results highlight the challenges in aligning scRNAseq data across cohorts and the need for multicenter investigations.

This study has notable strengths. Our study was designed to focus on a critical timepoint in CLAD pathogenesis. We were able to sequence 51,273 cells from 47 samples, which afforded ample power to identify rare subsets of cells. Another strength is in our design, where we focused purely on ALAD in the absence of infection or acute rejection, which is a common critical clinical problem that lacks a standard approach. In addition, our key findings were validated in 2 comparable external lung transplant cohorts.

One challenge of studying BAL is that most of the isolated cells are macrophages, which limits resolution to detect differences in lymphocyte and other myeloid populations. In addition, cell populations detectable by single cell transcriptomic approaches may be difficult to validate with traditional flow cytometry methods. Though, we are more confident in our results as we employed CITE-seq, which simultaneously quantifies both surface proteins and transcripts. Moreover, while we matched control samples to ALAD samples by time after transplantation, healthy recipients do not undergo routine bronchoscopy after the 2nd post-transplant year. Notably, we found no differences in key cell populations by time and almost all recipients were at their lowest post-transplant immunosuppression; though, there may be some residual bias reflecting differences in time after transplant.

We focused on 2 cell types of interest, but others were identified with potential biologic significance. We found increased T regulatory cells (Tregs) in association with progressive ALAD. While Tregs have been shown to be protective against CLAD in some studies, we and others have also shown an expansion of donor-reactive Tregs in association with acute rejection (48-51). Tregs proliferate in response to rejection associated cytokines and can thus reflect a protective compensatory response to acute inflammation.

There is currently no consensus guidance for the definition of ALAD, so our findings may not directly compare to prior studies using this term. Recipients in the ALAD-declined group developed CLAD based on how this group was defined, and so could be considered an early CLAD phenotype. However, this study did not include a referent group with late CLAD BAL samples. While explant tissue data suggest that some of the findings seen here could persist throughout the progression of CLAD, it is likely that other molecular features of CLAD evolve over time. Additional study of these cell populations is needed in both ACR and CLAD.

In conclusion, this CITE-seq study of ALAD after transplant identified 2 unique populations of cells with potential crosstalk that may be implicated in CLAD pathogenesis. Further work is needed to characterize these populations, which may reveal opportunities for therapeutic targeting.

Supplementary Material

Refer to Web version on PubMed Central for supplementary material.

ACKNOWLEDGEMENTS

We thank Jeffrey Golden, Mary Ellen Kleinhenz, Leslie Seijo, Julia Maheshwari, and the other members of the clinical lung transplant team for their care of our lung transplant patients and design of the clinical protocols. We thank the bronchoscopy technicians; Lindsey John, Naser Suleiman, and Justin Roasas Garrido, for assistance with sample collection. We thank Alexander Haile for his aid in processing and cataloging clinical samples. We are thankful for the cooperation of Donor Network West, for all the organ and tissue donors, and their families for giving gifts of life and knowledge with their generous donation.

This project was funded with support from ImmunoX. DRC receives salary support from the CFF (CALABR19Q0) and VA ORD BLRD (BX005301). JRG receives salary support from CFF (GREENL21AB0, HAYS19AB3, MCDYER22AB0), VA ORD (CX002011), and NIH (HL151552, HL161048, HL163294). The authors have no relevant disclosures to report.

DRC, JRG, and AC conceived and planned the experiments. DRC and CE performed the experiments. JPS, SRH, LEL, RJS, AV, NAK, JK, and AP contributed to sample collection and preparation. DRC, SY, CE, AC, and JRG performed data analysis and interpreted the results. DRC wrote the initial manuscript. All authors provided critical feedback and helped shape the research, analysis, and manuscript.

List of non-standard abbreviations:

ALAD	acute lung allograft dysfunction
BAL	Bronchoalveolar lavage
CITEseq	Cellular indexing of transcriptomes and epitopes (CITE) single cell sequencing
CLAD	Chronic lung allograft dysfunction
NK	Natural killer

REFERENCES

1. Chambers DC, Perch M, Zuckermann A, et al. : The International Thoracic Organ Transplant Registry of the International Society for Heart and Lung Transplantation: Thirty-eighth adult lung transplantation report - 2021; Focus on recipient characteristics. J Heart Lung Transplant 2021;40:1060–72. [PubMed: 34446355]
2. Graham CN, Watson C, Barlev A, Stevenson M, Dharnidharka VR: Mean lifetime survival estimates following solid organ transplantation in the US and UK. J Med Econ 2022;25:230–7. [PubMed: 35068310]
3. Venado A, Kukreja J, Greenland JR: Chronic Lung Allograft Dysfunction. Thorac Surg Clin 2022;32:231–42. [PubMed: 35512941]
4. Verleden GM, Glanville AR, Lease ED, et al. : Chronic lung allograft dysfunction: Definition, diagnostic criteria, and approaches to treatment-A consensus report from the Pulmonary Council of the ISHLT. J Heart Lung Transplant 2019;38:493–503. [PubMed: 30962148]
5. Tissot A, Danger R, Claustre J, Magnan A, Brouard S: Early Identification of Chronic Lung Allograft Dysfunction: The Need of Biomarkers. Front Immunol 2019;10:1681. [PubMed: 31379869]
6. Weigt SS, Wang X, Palchevskiy V, et al. : Gene Expression Profiling of Bronchoalveolar Lavage Cells Preceding a Clinical Diagnosis of Chronic Lung Allograft Dysfunction. PLoS One 2017;12:e0169894. [PubMed: 28103284]
7. Moshkelgosha S, Duong A, Wilson G, et al. : Interferon-stimulated and metallothionein-expressing macrophages are associated with acute and chronic allograft dysfunction after lung transplantation. The Journal of Heart and Lung Transplantation 2022;41:1556–69. [PubMed: 35691795]
8. Keller M, Sun J, Mutebi C, et al. : Donor-derived cell-free DNA as a composite marker of acute lung allograft dysfunction in clinical care. The Journal of Heart and Lung Transplantation 2022;41:458–66. [PubMed: 35063338]
9. Royer PJ, Olivera-Botello G, Koutsokera A, et al. : Chronic Lung Allograft Dysfunction: A Systematic Review of Mechanisms. Transplantation 2016;100:1803–14. [PubMed: 27257997]
10. Verleden GM, Raghu G, Meyer KC, Glanville AR, Corris P: A new classification system for chronic lung allograft dysfunction. J Heart Lung Transplant 2014;33:127–33. [PubMed: 24374027]
11. Verleden SE, Vos R, Vanaudenaerde BM, Verleden GM: Chronic lung allograft dysfunction phenotypes and treatment. J Thorac Dis 2017;9:2650–9. [PubMed: 28932572]
12. Naikawadi RP, Green G, Jones KD, et al. : Airway Epithelial Telomere Dysfunction Drives Remodeling Similar to Chronic Lung Allograft Dysfunction. Am J Respir Cell Mol Biol 2020;63:490–501. [PubMed: 32551854]

13. Sacreas A, Yang JYC, Vanaudenaerde BM, et al. : The common rejection module in chronic rejection post lung transplantation. PLoS One 2018;13:e0205107. [PubMed: 30289917]
14. Calabrese DR, Chong T, Wang A, et al. : NKG2C Natural Killer Cells in Bronchoalveolar Lavage Are Associated With Cytomegalovirus Viremia and Poor Outcomes in Lung Allograft Recipients. Transplantation 2019;103:493–501. [PubMed: 30211828]
15. Calabrese DR, Chong T, Singer JP, et al. : CD16(+) natural killer cells in bronchoalveolar lavage are associated with antibody-mediated rejection and chronic lung allograft dysfunction. Am J Transplant 2023;23:37–44. [PubMed: 36695619]
16. Greenland JR, Wong CM, Ahuja R, et al. : Donor-Reactive Regulatory T-Cell Frequency Increases During Acute Cellular Rejection of Lung Allografts. Transplantation 2016.
17. Snyder ME, Finlayson MO, Connors TJ, et al. : Generation and persistence of human tissue-resident memory T cells in lung transplantation. Sci Immunol 2019;4.
18. Todd JL, Neely ML, Kopetskie H, et al. : Risk Factors for Acute Rejection in the First Year after Lung Transplant: A Multicenter Study. Am J Respir Crit Care Med 2020.
19. Balthesen M, Dreher L, Lučin P, Reddehase MJ: The establishment of cytomegalovirus latency in organs is not linked to local virus production during primary infection. J Gen Virol 1994;75:2329–36. [PubMed: 8077931]
20. Hodge G, Hodge S, Yeo A, et al. : BOS Is Associated With Increased Cytotoxic Proinflammatory CD8 T, NKT-Like, and NK Cells in the Small Airways. Transplantation 2017;101:2469–76. [PubMed: 28926522]
21. Ward C, Whitford H, Snell G, et al. : Bronchoalveolar lavage macrophage and lymphocyte phenotypes in lung transplant recipients. J Heart Lung Transplant 2001;20:1064–74. [PubMed: 11595561]
22. West EE, Lavoie TL, Orens JB, et al. : Pluripotent Allospecific CD8+ Effector T Cells Traffic to Lung in Murine Obliterative Airway Disease. Am J Respir Cell Mol Biol 2006;34:108–18. [PubMed: 16195540]
23. Liu Z, Liao F, Zhu J, et al. : Reprogramming alveolar macrophage responses to TGF-β reveals CCR2+ monocyte activity that promotes bronchiolitis obliterans syndrome. The Journal of Clinical Investigation 2022;132.
24. Calabrese DR, Florez R, Dewey K, et al. : Genotypes associated with tacrolimus pharmacokinetics impact clinical outcomes in lung transplant recipients. Clin Transplant 2018;32:e13332. [PubMed: 29920787]
25. Combes AJ, Courau T, Kuhn NF, et al. : Global absence and targeting of protective immune states in severe COVID-19. Nature 2021;591:124–30. [PubMed: 33494096]
26. Nestorowa S, Hamey FK, Pijuan Sala B, et al. : A single-cell resolution map of mouse hematopoietic stem and progenitor cell differentiation. Blood 2016;128:e20–e31. [PubMed: 27365425]
27. Calabrese DR, Tsao T, Magnen M, et al. : NKG2D receptor activation drives primary graft dysfunction severity and poor lung transplantation outcomes. JCI Insight 2022;7:e164603. [PubMed: 36346670]
28. Khatri A, Todd JL, Kelly FL, et al. : JAK-STAT activation contributes to cytotoxic T cell–mediated basal cell death in human chronic lung allograft dysfunction. JCI Insight 2023;8.
29. Kuhn M, Johnson K: Applied Predictive Modeling: Springer; 2013.
30. Diamond JM, Lee JC, Kawut SM, et al. : Clinical risk factors for primary graft dysfunction after lung transplantation. Am J Respir Crit Care Med 2013;187:527–34. [PubMed: 23306540]
31. Lederer DJ, Bell SC, Branson RD, et al. : Control of Confounding and Reporting of Results in Causal Inference Studies. Guidance for Authors from Editors of Respiratory, Sleep, and Critical Care Journals. Ann Am Thorac Soc 2019;16:22–8. [PubMed: 30230362]
32. Nahrendorf M, Swirski FK: Abandoning M1/M2 for a Network Model of Macrophage Function. Circ Res 2016;119:414–7. [PubMed: 27458196]
33. Ni Y, Wu GH, Cai JJ, et al. : Tubule-mitophagic secretion of SerpinG1 reprograms macrophages to instruct anti-septic acute kidney injury efficacy of high-dose ascorbate mediated by NRF2 transactivation. Int J Biol Sci 2022;18:5168–84. [PubMed: 35982894]

34. Schraufstatter IU, Zhao M, Khaldoyanidi SK, Discipio RG: The chemokine CCL18 causes maturation of cultured monocytes to macrophages in the M2 spectrum. Immunology 2012;135:287–98. [PubMed: 22117697]
35. Yan C, Lian X, Li Y, et al. : Macrophage-specific expression of human lysosomal acid lipase corrects inflammation and pathogenic phenotypes in lal−/− mice. Am J Pathol 2006;169:916–26. [PubMed: 16936266]
36. Ennis S, Jomary C, Mullins R, et al. : Association between the SERPING1 gene and age-related macular degeneration: a two-stage case–control study. The Lancet 2008;372:1828–34.
37. Weigt SS, Wang X, Palchevskiy V, et al. : Usefulness of gene expression profiling of bronchoalveolar lavage cells in acute lung allograft rejection. J Heart Lung Transplant 2019.
38. Dugger DT, Fung M, Hays SR, et al. : Chronic lung allograft dysfunction small airways reveal a lymphocytic inflammation gene signature. Am J Transplant 2021;21:362–71. [PubMed: 32885581]
39. Kok L, Masopust D, Schumacher TN: The precursors of CD8+ tissue resident memory T cells: from lymphoid organs to infected tissues. Nature Reviews Immunology 2022;22:283–93.
40. Uddbäck I, Cartwright EK, Schøller AS, et al. : Long-term maintenance of lung resident memory T cells is mediated by persistent antigen. Mucosal Immunol 2021;14:92–9. [PubMed: 32518368]
41. Wein AN, McMaster SR, Takamura S, et al. : CXCR6 regulates localization of tissue-resident memory CD8 T cells to the airways. J Exp Med 2019;216:2748–62. [PubMed: 31558615]
42. Snyder ME, Moghbeli K, Bondonese A, et al. : Modulation of tissue resident memory T cells by glucocorticoids after acute cellular rejection in lung transplantation. J Exp Med 2022;219.
43. Yanagihara T, Hata K, Suzuki K, et al. : Expansion of ST2-expressing macrophages in a patient with bronchiolitis obliterans syndrome. ERJ Open Research 2023;9:00033–2023. [PubMed: 37260458]
44. Snyder ME, Sembrat J, Noda K, et al. : Human Lung-Resident Macrophages Colocalize with and Provide Costimulation to PD1hi Tissue-Resident Memory T Cells. Am J Respir Crit Care Med 2020;203:1230–44.
45. Grant RA, Morales-Nebreda L, Markov NS, et al. : Circuits between infected macrophages and T cells in SARS-CoV-2 pneumonia. Nature 2021;590:635–41. [PubMed: 33429418]
46. Bos S, Filby AJ, Vos R, Fisher AJ: Effector immune cells in chronic lung allograft dysfunction: A systematic review. Immunology 2022;166:17–37. [PubMed: 35137398]
47. Ghio AJ, Sangani RG, Brighton LE, Carson JL: MRT letter: Auto-fluorescence by human alveolar macrophages after in vitro exposure to air pollution particles. Microsc Res Tech 2010;73:579–82. [PubMed: 19941295]
48. Salman J, Ius F, Knoefel AK, et al. : Association of Higher CD4(+) CD25(high) CD127(low) , FoxP3(+) , and IL-2(+) T Cell Frequencies Early After Lung Transplantation With Less Chronic Lung Allograft Dysfunction at Two Years. Am J Transplant 2017;17:1637–48. [PubMed: 27931084]
49. Bhorade SM, Chen H, Molinero L, et al. : Decreased percentage of CD4+FoxP3+ cells in bronchoalveolar lavage from lung transplant recipients correlates with development of bronchiolitis obliterans syndrome. Transplantation 2010;90:540–6. [PubMed: 20628341]
50. Greenland JR, Wong CM, Ahuja R, et al. : Donor-Reactive Regulatory T Cell Frequency Increases During Acute Cellular Rejection of Lung Allografts. Transplantation 2016;100:2090–8. [PubMed: 27077597]
51. Durand M, Lacoste P, Danger R, et al. : High circulating CD4+CD25hiFOXP3+T-cell sub-population early after lung transplantation is associated with development of bronchiolitis obliterans syndrome. The Journal of Heart and Lung Transplantation.

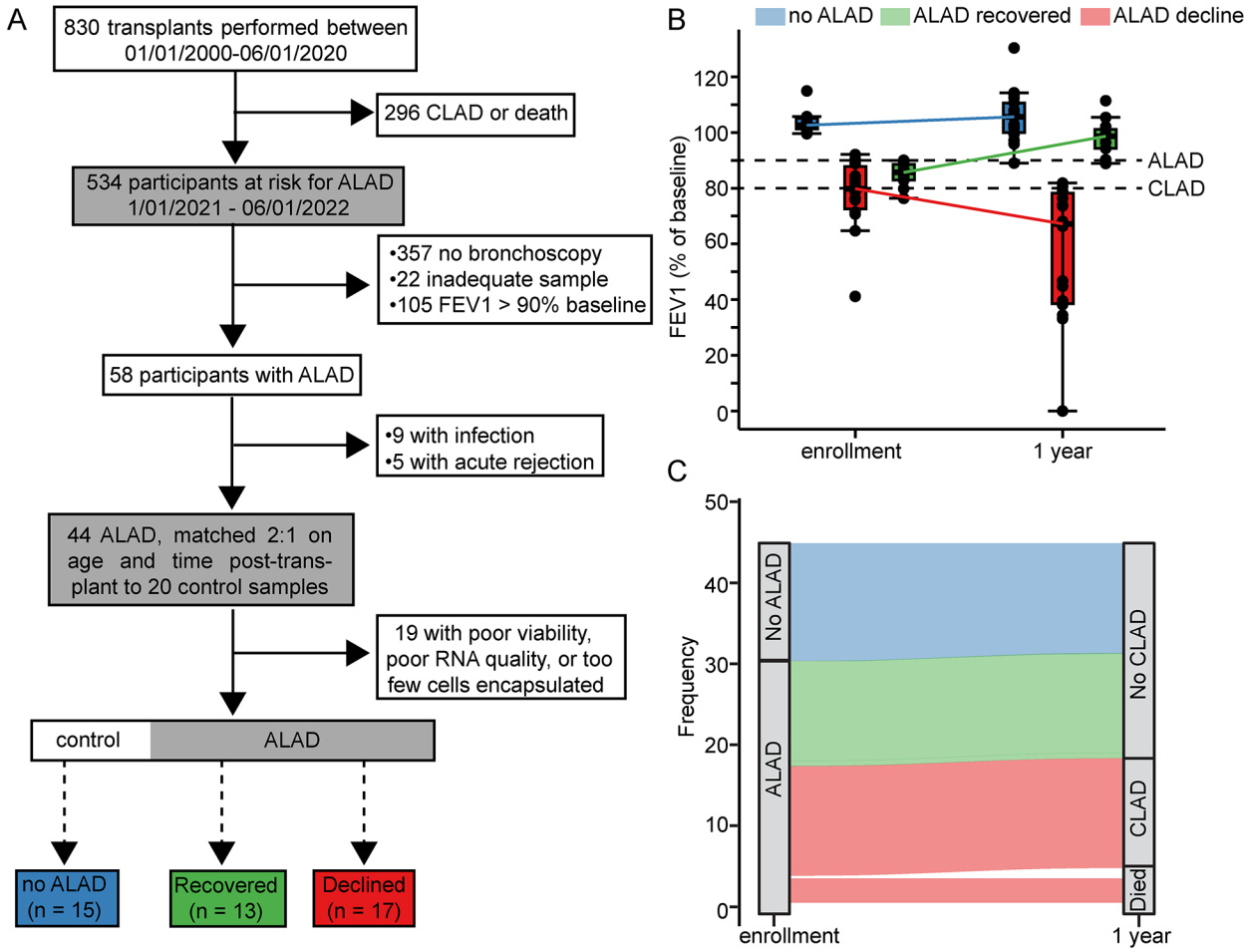

Figure 1. Participant recruitment and clinical outcomes.

(A) Lung transplant recipients were included who underwent bronchoscopy at a single institution and had sufficient sample available. Acute lung allograft dysfunction (ALAD) was defined as a 10% decrease in participants without pre-existing Chronic Lung Allograft Dysfunction (CLAD) and in the absence of infection or acute rejection. Participants with ALAD were matched 2:1 on age and time after transplant with no-ALAD control participants. **(B)** Stratification of study participants by FEV1 at the time of enrollment and at 1 year follow-up. **(C)** Alluvial diagram demonstrating outcomes for each of the participants' samples. Note that 2 ALAD participants had "control" samples available from a period of stability preceding their ALAD events.

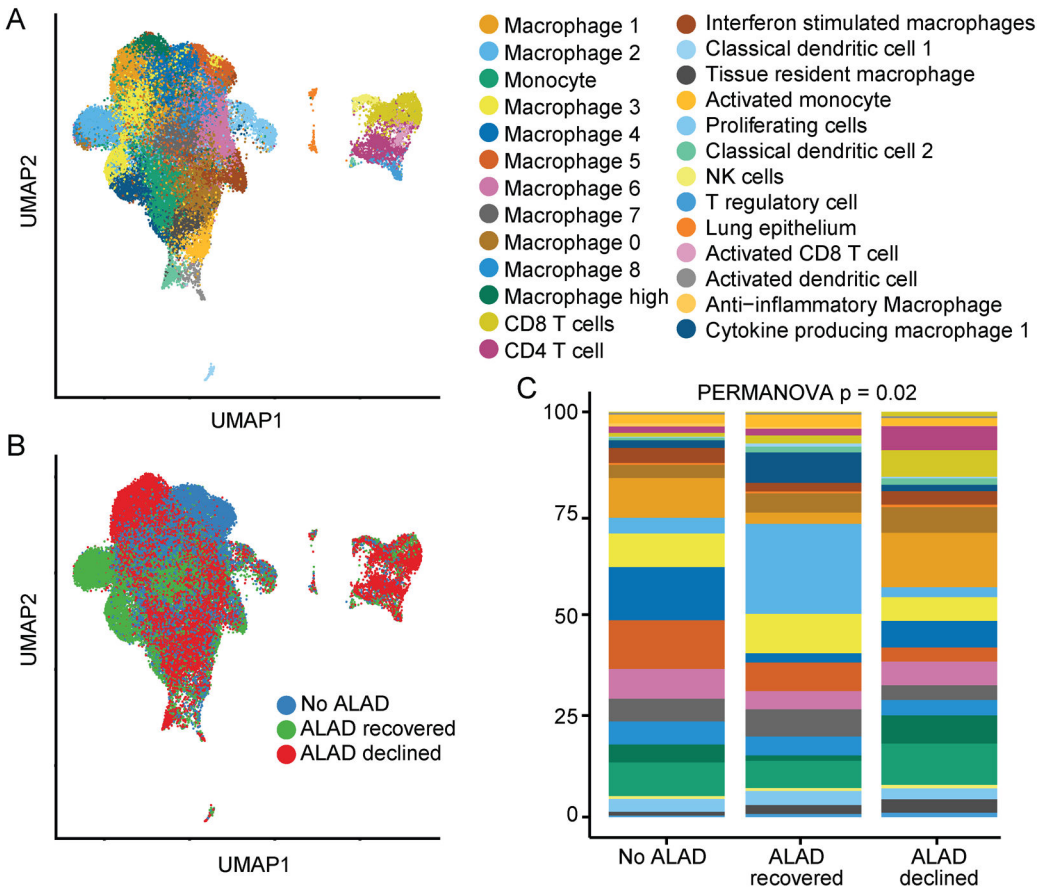

Figure 2. Cell populations in the bronchoalveolar lavage.

We performed dimensionality reduction using Uniform Manifold Approximation and Projection (UMAP) and semi-supervised clustering of BAL scRNAseq. **(A)** UMAP of the 26 distinct cell clusters in the BAL across groups. **(B)** UMAP shaded by ALAD status. **(C)** Bar plots of frequencies of individual clusters across the 3 ALAD groupings. Comparisons of proportions of cell frequency differences across ALAD groups were made using PERMANOVA.

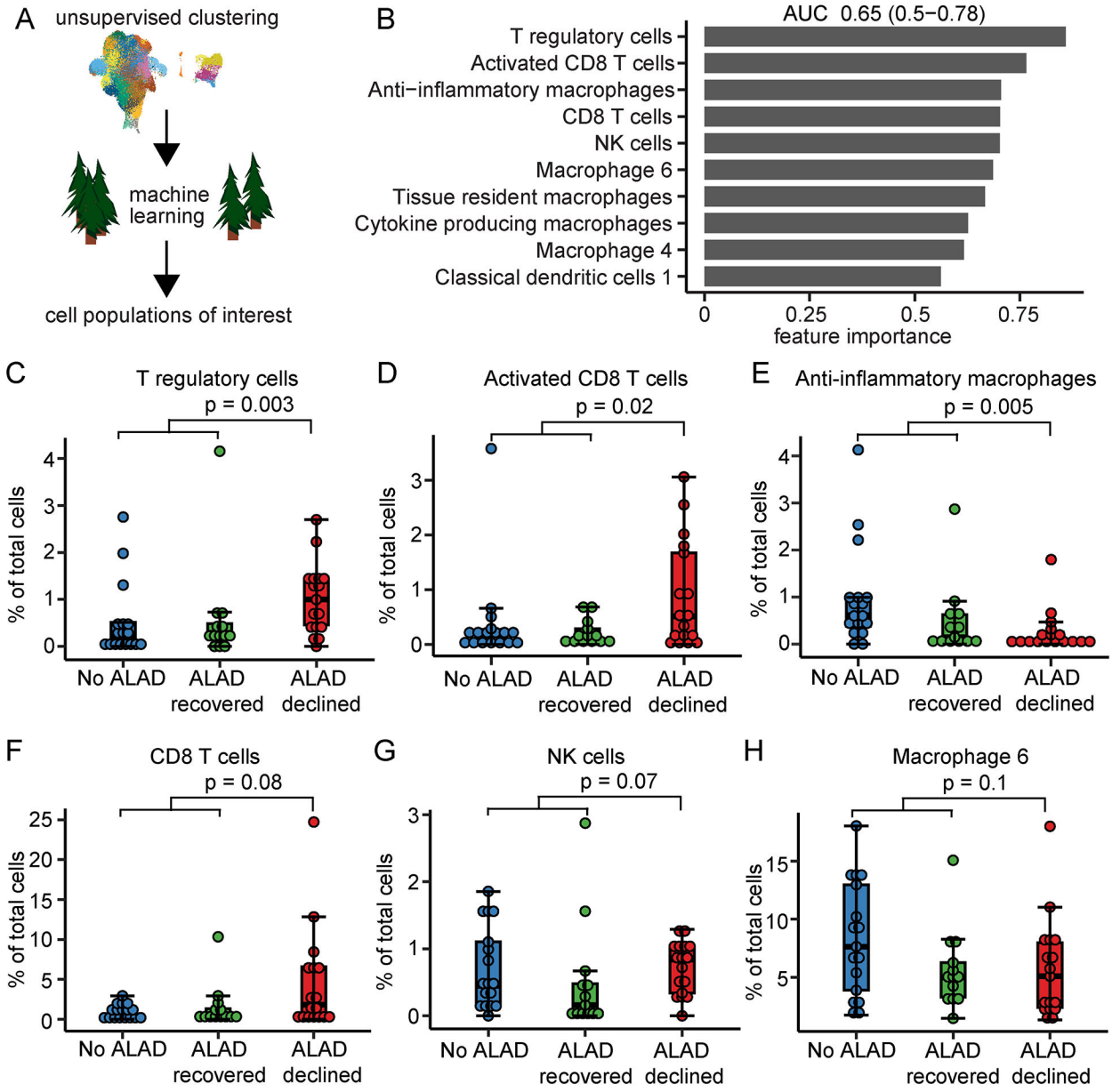

Figure 3. Lymphocytes and macrophages identify ALAD progression.

(A) A random forest machine learning model was generated to determine which of the 26 cell cluster frequencies predicted ALAD decline (n = 17) as compared to the no ALAD (n = 17) and ALAD recovered (n = 13) groups. **(B)** Relative feature importance of the individual clusters from the machine learning model with an area under the curve (AUC) fit of 0.65 (95% Confidence Interval 0.5 – 0.78). We show individual cell cluster frequencies for the top 6 populations by feature importance: (**C)** T regulatory cells, **(D)** Activated CD8 T cells, **(E)** Anti-inflammatory macrophages, **(F)** CD8 T cells, **(G)** NK cells, and **(H)** Macrophage 6. Box and whisker plots display individual data points bound by boxes at 25th and 75th percentiles and medians depicted with bisecting lines. Differences were assessed using the Mann-Whitney U test with $p<0.05$ considered significant.

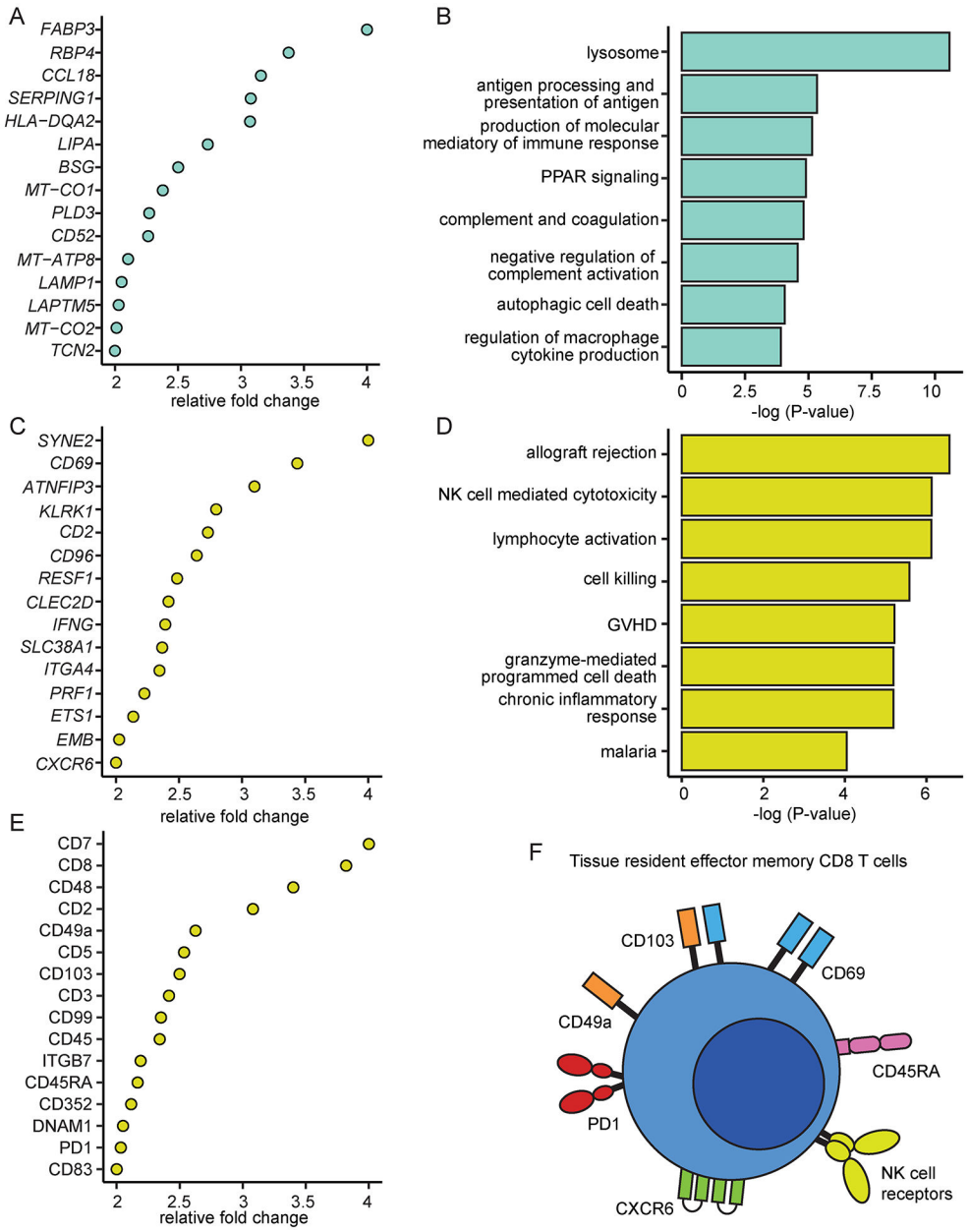

Figure 4. Anti-inflammatory macrophage and activated CD8 T cell profiling.

We sought to identify the functional profiles of these 2 cell clusters (**A**). The top 15 differentially expressed genes in anti-inflammatory macrophages. (**B**) Results from the pathway analysis of these transcripts. **(C**). The top 15 differentially expressed genes defining the activated CD8 T cell cluster. (**D)** Results from the pathway analysis of these CD8 T cell genes. **(E**) The top 15 surface markers in the activated CD8 T cell cluster. (**F**) Activated CD8 T cells show transcriptional and surface expression of markers consistent with a tissue resident effector memory (TREM) phenotype. The top differentially transcribed genes and surface markers were defined by false discovery rate (FDR) p-values < 0.05 and stratified by relative fold change.

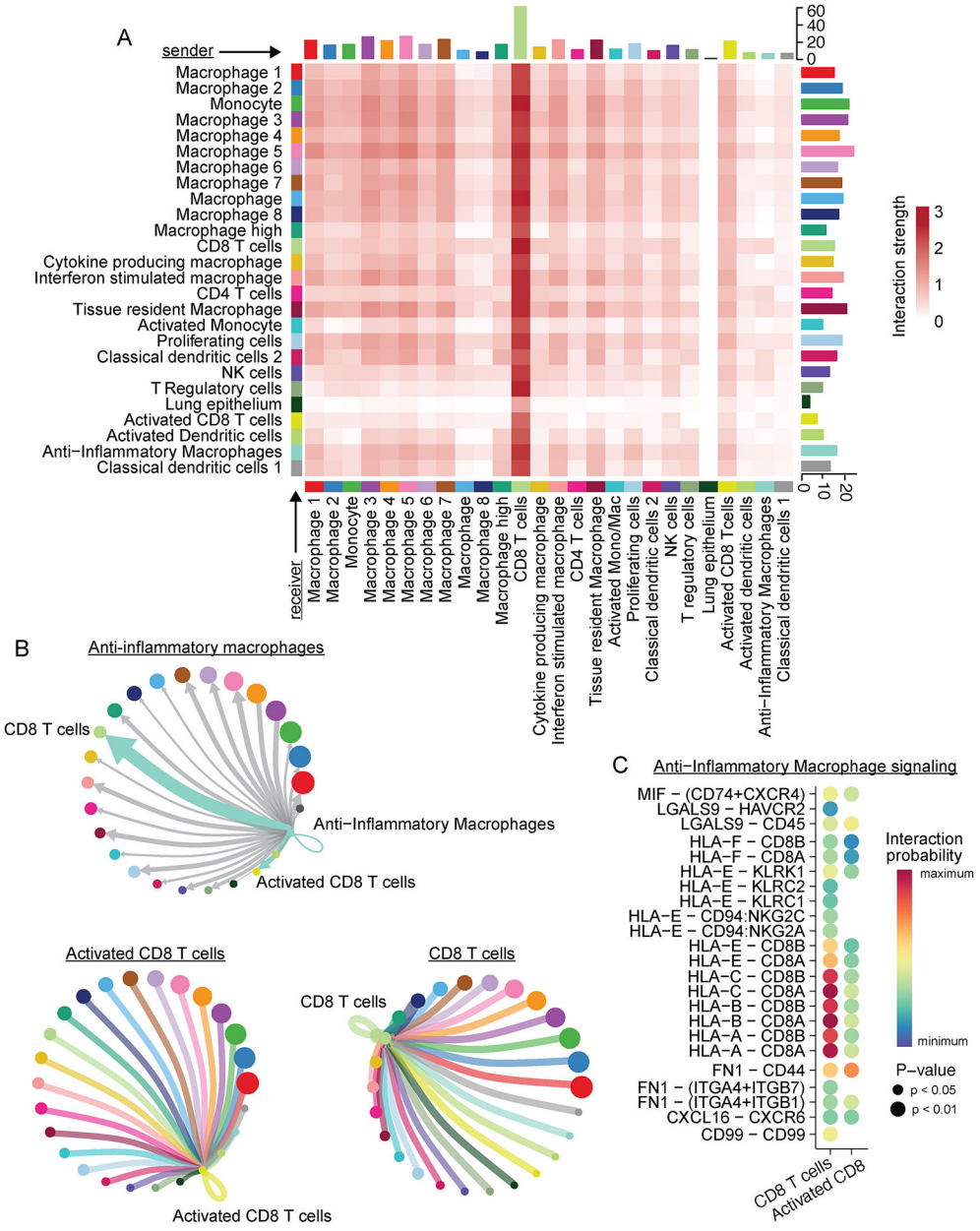

Figure 5. Cell communication across cluster landscape.

We modeled the interaction strength between the cell clusters across the cohort based on predicted receptor and ligand pairings. **(A)** There was significant cell communication across cell clusters. **(B)** Anti-inflammatory macrophages and CD8 T cell cluster signal direction and interaction strength. Anti-inflammatory macrophages had out-going signals with significant transduction to CD8 and Activated CD8 T cells. The CD8 T cells had in-coming signals from all other populations. **(C)** Predicted ligand-receptor interactions between anti-inflammatory macrophages and CD8 T cells.

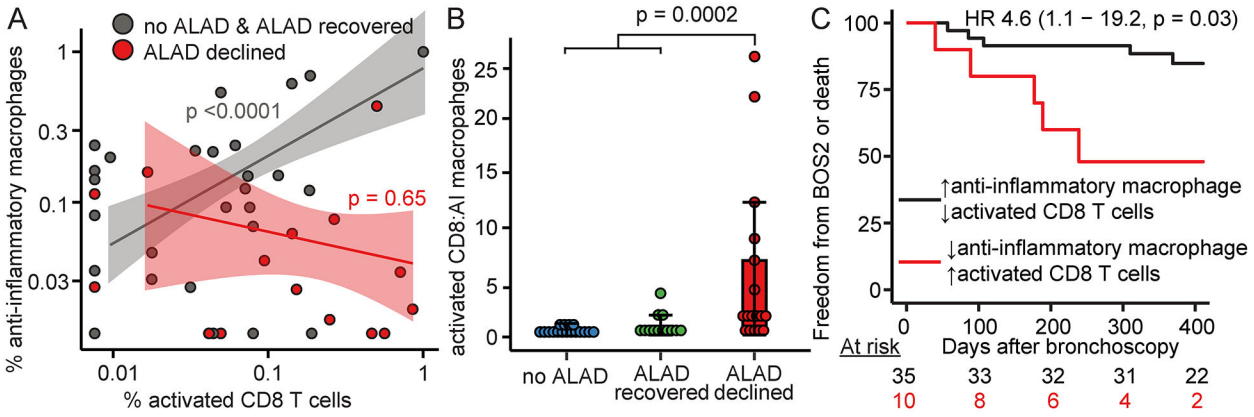

Figure 6. Discordance in anti-inflammatory macrophages and activated CD8 T cells predicts allograft failure.

(A) Scatter plot of activated CD8 T cells and anti-inflammatory macrophages colored by ALAD status with lines fit via linear regression. **(B)** Ratio of counts of activated CD8 T cells to anti-inflammatory macrophages in ALAD groups. **(C)** Kaplan Meier plot recipients with high activated CD8 T cells (> median) and low anti-inflammatory macrophages (<median, n = 10) compared to recipients without this cellular discordance (n = 35). P-values determined by (A) linear regression, (B) Mann-Whitney U Test, and (C) Cox Proportional Hazards. Box and whisker plot displays individual data points bound by boxes at 25th and 75th percentiles and medians depicted with bisecting lines.

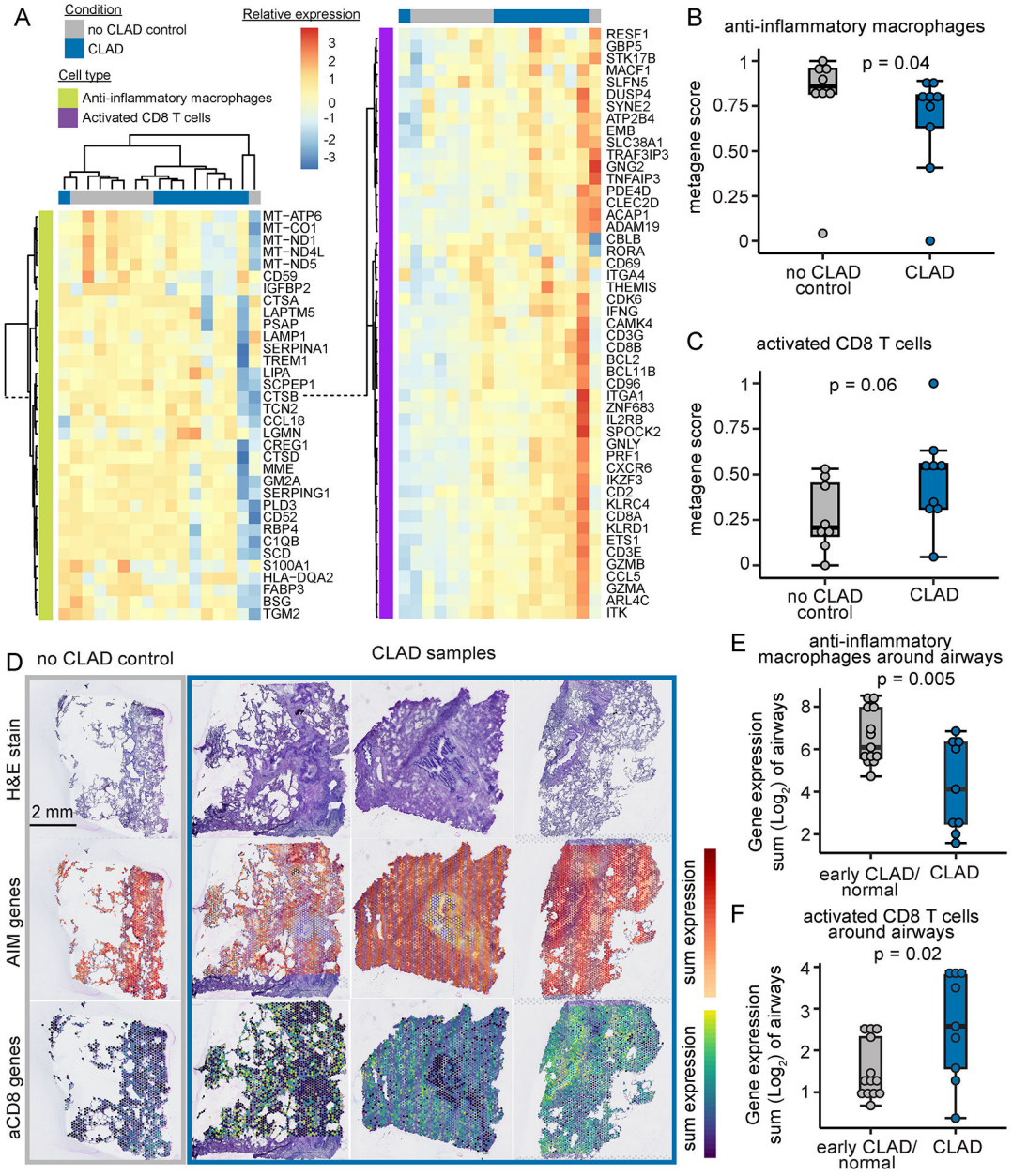

Figure 7. Validation of findings in two separate lung transplant cohorts.

Within an existing BAL sequencing cohort of no CLAD participants (n = 8) and participants with incipient CLAD (n = 9), we constructed metagene scores for anti-inflammatory macrophages (AIM) and activated CD8 T cells (aCD8). (**A)** A heatmap showing the relative expression of the gene score components by cell cluster type. **(B)** Anti-inflammatory macrophage gene score was decreased in CLAD BAL. (**C)** Activated CD8 T cell gene score was numerically increased in CLAD BAL. Separately, in a tissue gene expression cohort of CLAD tissue (n = 3) and no CLAD tissue (n = 1), we measured the same gene expression in these 2 cell clusters (**D).** Around CLAD airways, anti-inflammatory macrophage genes were decreased **(E)** and activated CD8 T cells were increased as compared to no CLAD airways. Box and whisker plot displays individual data points bound by boxes at 25th and

75^{th} percentiles and medians depicted with bisecting lines. Comparisons in gene scores across CLAD conditions were made using Mann-Whitney U tests in the BAL cohort and linear regression modeling sample as a random effect.

Table 1.

Cohort characteristics of ALAD and non-ALAD control recipients

	No ALAD (N = 15)	ALAD (N = 30)	P value
Sex, Male N (%)	9 (60)	19 (63.3)	1
Age, Mean ± SD)	51.9 ± 16.1	57 ± 10.7	0.28
Diagnosis, N (%)			0.46
ILD	10 (66.7)	26 (86.7)	
COPD	1 (6.7)	1 (3.3)	
CF	1 (6.7)	1 (3.3)	
pHTN	3 (20)	9 (6.7)	
Race, N (%)			0.82
Caucasian	8 (53.3)	18 (60)	
African American	2 (13.3)	3 (10)	
Hispanic	5 (33.3)	7 (23.3)	
Asian	0 (0)	1 (3.3)	
Other	0 (4.5)	1 (3.3)	
Transplant Type, N (%)			1
Single	1 (6.7)	1 (3.3)	
Bilateral	14 (93.3)	29 (96.7)	
Sample time, N (%)			0.45
6-12 months	2 (13.3)	2 (6.7)	
12-18 months	3 (20)	7 (23.3)	
18-24 months	5 (33.3)	5 (16.7)	
>24 months	5 (33.3)	16 (53.3)	